J|A|C|S
ARTICLES

Published on Web 01/15/2009

Highly Stable Crystalline Catalysts Based on a Microporous Metal−Organic Framework and Polyoxometalates

Chun-Yan Sun, Shu-Xia Liu,* Da-Dong Liang, Kui-Zhan Shao, Yuan-Hang Ren, and Zhong-Min Su*

Key Laboratory of Polyoxometalate Science of Ministry of Education, College of Chemistry, Northeast Normal University, Changchun, Jilin 130024, China

Received September 17, 2008; E-mail: liusx@nenu.edu.cn

Abstract: A series of remarkable crystalline compounds $[Cu_2(BTC)_{4/3}(H_2O)_2]_6[H_nXM_{12}O_{40}]\cdot(C_4H_{12}N)_2$ (X = Si, Ge, P, As; M = W, Mo) were obtained from the simple one-step hydrothermal reaction of copper nitrate, benzentricaboxylate (BTC), and different Keggin polyoxometalates (POMs). In these compounds, the catalytically active Keggin polyanions were alternately arrayed as noncoordinating guests in the cuboctahedral cages of a Cu-BTC-based metal−organic framework (MOF) host matrix. X-ray crystallographic analyses, TG, FT-IR, UV−vis, N_2 adsorption studies, and acid−base titration demonstrated their high stability and toleration for thermal and acid−base conditions. No POM leaching or framework decomposition was observed in our study. The representative acid catalytic performance of a compound containing PW_{12} species was assessed through the hydrolysis of esters in excess water, which showed high catalytic activity and can be used repeatedly without activity loss. Moreover, catalytic selectivity, which is dependent on the molecular size of substrates, and substrate accessibility for the pore surface were observed. It is the first time that the well-defined, crystalline, MOF-supported POM compound has behaved as a true heterogeneous acid catalyst. The unique attributes of MOF and well-dispersed level of POMs prohibited the conglomeration and deactivation of POMs, which allowed for the enhancement of their catalytic properties.

Introduction

The design of active, selective, environmentally benign, and recyclable heterogeneous catalysts is expected to have a major impact on industrial applications. Polyoxometalates (POMs) have received increasing attention because of their numerous advantageous properties.[1] The POMs with strong Brønsted acidity show promise as solid-acid catalysts for many acid-catalyzed organic transformations and industrial applications, such as the hydration of alkenes, esterification, and alkylation.[2−6] The pure bulk POMs present relatively small surface areas (<10 m^2 g^{-1}) that hinder accessibility to the active sites. Therefore, the applications of POMs as solid catalysts are limited. Thus, various high-surface-area supports, such as silica,[7] activated carbon,[8] ion-exchange resin,[9] and mesoporous molecular sieves,[10] have been used for POMs dispersion. However, these systems are often regarded as ill-defined with many limitations, including low POM loading, POM leaching, the conglomeration of POM particles, active sites that are nonuniform, and the deactivation of acid sites by water. The immobilization of POMs in a suitable solid matrix, which can overcome these drawbacks, is a step toward the challenging goal of catalysis.

An optimum host matrix supporting POMs should possess several attributes: (i) suitable cavities with the proper size and shape for the encapsulation of one guest POMs molecule per

(1) (a) Hussain, F.; Kortz, U.; Keita, B.; Nadjo, L.; Pope, M. T. *Inorg. Chem.* **2006**, *45*, 761. (b) Liu, T.; Imber, B.; Diemann, E.; Liu, G.; Cokleski, K.; Li, H.; Chen, Z.; Müller, A. *J. Am. Chem. Soc.* **2006**, *128*, 15914. (c) Geletii, Y. V.; Hill, C. L.; Atalla, R. H.; Weinstock, I. A. *J. Am. Chem. Soc.* **2006**, *128*, 17033. (d) Uchida, S.; Kawamoto, R.; Tagami, H.; Nakagawa, Y.; Mizuno, N. *J. Am. Chem. Soc.* **2008**, *130*, 12370. (e) Cadot, E.; Pouet, M.-J.; Robert-Labarre, C.; du Peloux, C.; Marrot, J.; Sécheresse, F. *J. Am. Chem. Soc.* **2004**, *126*, 9127. (f) Long, D.-L.; Streb, C.; Song, Y.-F.; Mitchell, S.; Cronin, L. *J. Am. Chem. Soc.* **2008**, *130*, 1830. (g) Zheng, S.-T.; Zhang, J.; Yang, G.-Y. *Angew. Chem., Int. Ed.* **2008**, *47*, 3909. (h) Wang, C.-M.; Zheng, S.-T.; Yang, G.-Y. *Inorg. Chem.* **2007**, *46*, 616. (i) Li, T.; Li, F.; Lü, J.; Guo, Z.; Gao, S.; Cao, R. *Inorg. Chem.* **2008**, *47*, 5612. (j) Kong, X.-J.; Ren, Y.-P.; Zheng, P.-Q.; Long, Y.-X.; Long, L.-S.; Huang, R.-B.; Zheng, L.-S. *Inorg. Chem.* **2006**, *45*, 10702.

(2) Ono, Y. In *Perspectives in Catalysis*; Thomas, J. M.; Zamaraev, K. I., Eds.; Blackwell: London, 1992; p 341.

(3) (a) Kozhevnikov, I. V. *Russ. Chem. Rev.* **1987**, *56*, 811. (b) Lefebvre, F.; Liu-Cai, F. X.; Auroux, A. *J. Mater. Chem.* **1994**, 125.

(4) (a) Misono, M. *Catal. Rev. Sci. Eng.* **1987**, *29*, 269. (b) Misono, M. *Catal. Rev. Sci. Eng.* **1988**, *30*, 339.

(5) Izumi, Y.; Urabe, K.; Onaka, M. *Zeolite, Clay and Heteropoly Acid in Organic Reactions*; Kodansha/VCH: Tokyo, 1992; p 99.

(6) (a) Kozhevnikov, I. V. *Catal. Rev. Sci. Eng.* **1995**, *37*, 311. (b) Kozhevnikov, I. V. *Chem. Rev.* **1998**, *98*, 171. (c) Okuhara, T.; Mizuno, N.; Misono, M. *Adv. Catal.* **1995**, *41*, 113.

(7) (a) Lefebvre, F. *J. Chem. Soc., Chem. Commun.* **1992**, 756. (b) Kozhevnikov, I. V.; Kloetstra, K. R.; Sinnema, A.; Zandbergen, H. W.; Van Bekkum, H. *J. Mol. Catal. A* **1996**, *114*, 287. (c) Guo, Y.; Wang, Y.; Hu, C.; Wang, Y.; Wang, E. *Chem. Mater.* **2000**, *12*, 3501. (d) Peng, G.; Wang, Y.; Hu, C. *Appl. Catal., A* **2001**, *218*, 91. (e) Guo, Y.; Hu, C. *J. Mol. Catal. A* **2007**, *262*, 136.

(8) (a) Gall, R. D.; Hill, C. L.; Walker, J. E. *Chem. Mater.* **1996**, *8*, 2523. (b) Watson, B. A.; Barteau, M. A.; Haggerty, L.; Lenhoff, A. M.; Weber, R. S. *Langmuir* **1992**, *8*, 1145.

(9) Schwegler, M. A.; Van Bekkum, H.; de Munck, N. A. *Appl. Catal.* **1991**, *74*, 191.

(10) (a) Kresge, C. T.; Leonowicz, M. E.; Roth, W. J.; Vartuli, J. C.; Beck, J. S. *Nature* **1992**, *359*, 710. (b) Blasco, T.; Corma, A.; Martinez, A.; Martinez-Escolano, P. *J. Catal.* **1998**, *177*, 306. (c) Kozhevnikov, I. V.; Sinnema, A.; Jansen, R. J. J.; Pamin, K.; Van Bekkum, H. *Catal. Lett.* **1995**, *30*, 241. (d) Zhao, D.; Feng, J.; Huo, Q.; Melosh, N.; Fredrickson, G. H.; Chmelka, B. F.; Stucky, G. D. *Science* **1998**, *279*, 548.

 © 2009 American Chemical Society

cavity, thus allowing the dispersion of POMs at the molecular level; (ii) appropriate openings allowing for the diffusion of reactants and products; (iii) mild and simple synthesis conditions permitting the one-step framework construction and encapsulation of the guest POMs; and (iv) a framework with integrity and stability. Bearing these thoughts in mind, metal−organic frameworks (MOFs),[11] which have the potential to meet these criteria, can be used as host matrices to encapsulate POMs and form a series of unique, tunable catalysts.

Today, the major impetus to advance MOF exploitation extends beyond charming architecture to the development of new strategies for constructing made-to-order MOFs as platforms for a desired application. MOFs have emerged as a particular class of functional solid-state materials, owing to their applications in gas storage,[12] separation,[13] catalysis,[14] and drug delivery.[15] An especially notable characteristic of some MOFs is their extra-large cavity, which enables their exploration in applications composed of large molecules, like drugs,[15] dyes,[16] metalloporphyrin molecules,[17] and even the nanosized POMs clusters. Several compounds that POMs were introduced into the MOF segments have been reported.[18] However, highly efficient, truly heterogeneous catalysis over well-defined POM/MOF materials had not been presented until now. Maksimchuk et al.[19] recently demonstrated that these systems could be utilized as oxidation catalysts, but they did not determine their crystal structures. These catalysts were constructed with coordination polymer MIL-101 and transition metal substituted POMs and characterized by elemental analysis and spectroscopy.

Here we present the preparation and catalysis of a series of new crystalline catalysts, $[Cu_2(BTC)_{4/3}(H_2O)_2]_6[POM]\cdot(C_4H_{12}N)_2\cdot xH_2O$, which are denoted, respectively, as **NENU-*n*** (Northeast Normal University, $n = 1-6$; BTC = 1,3,5-benzentricaboxylate); POM = $[H_2SiW_{12}O_{40}]^{2-}$ (**1**); $[H_2GeW_{12}O_{40}]^{2-}$ (**2**); $[HPW_{12}O_{40}]^{2-}$ (**3**); $[H_2SiMo_{12}O_{40}]^{2-}$ (**4**); $[HPMo_{12}O_{40}]^{2-}$ (**5**); $[HAsMo_{12}O_{40}]^{2-}$ (**6**) ($x = 25-30$) in which the Keggin-type POMs are incorporated into an open system of an MOF through a one-step hydrothermal reaction. Although **3** and **4** have been synthesized previously by Yang et al.,[18d] who used Na_2WO_4, NaH_2PO_4, Na_2MoO_4, and Na_2SiO_3 as starting materials, reporting only the crystal structures, we used the Keggin-type POMs as the precursor to obtaining a similar structure with high purity and yields. Considering the importance of these two compounds as catalysts and the system of study, they are also listed. We adopted the Keggin-type POMs and the MOF comprised of metal carboxylate SBUs for the following two reasons: the Keggin-type POMs are widely used as catalysts due to their very strong Brønsted acidity and special structural properties;[6] and the rigid metal carboxylate SBUs usually lead to the formation of stable frameworks.[20] Accordingly, we successfully prepared a series of compounds based on the charge-neutral Cu-BTC host framework and Keggin-type polyoxometalates which served as guests and filled in the pores.

Experimental Section

Materials and Instruments. All chemicals were obtained commercially and used without additional purification. The $H_4SiW_{12}O_{40}\cdot nH_2O$, $H_4SiMo_{12}O_{40}\cdot nH_2O$, $H_4GeW_{12}O_{40}\cdot nH_2O$, $H_3AsMo_{12}O_{40}\cdot nH_2O$, $H_3PW_{12}O_{40}\cdot nH_2O$, and $H_3PMo_{12}O_{40}\cdot nH_2O$ precursors were synthesized according to the procedure described in the literature[21] and characterized by IR spectra. For comparison, the host matrix (HKUST-**1**) was also prepared as described by Chui et al.[22] and characterized by IR and XRD spectra.

Elemental analyses (C, H, and N) were performed on a Perkin-Elmer 2400 CHN elemental analyzer, and W, Mo, Cu, Si, Ge, As, and P were determined with a PLASMA-SPEC(I) ICP atomic emission spectrometer. IR spectra were recorded in the range 400−4000 cm^{-1} on an Alpha Centaurt FT/IR spectrophotometer using KBr pellets. Thermal gravimetric (TG) analyses were performed on a Perkin-Elmer TGA7 instrument in flowing N_2 with a heating rate of 10 °C/min. Powder X-ray diffraction (XRD) measurements were performed on a Rigaku D/MAX-3 instrument with Cu Kα radiation in the angular range $2\theta = 3°-50°$ at 293 K. The leakage of POM species from the framework into the liquid phase was estimated by measuring the UV absorption characteristics of the Keggin anion (260−270 nm) on a 756 CRT UV−vis spectrophotometer. A Micromeritics ASAP 2010 surface area and porosity analyzer was used to measure N_2 sorption. The products of catalysis experiments were analyzed with a GC (Agilent 6890N instrument) and GC−MS (Agilent 5975/6890).

Syntheses of NENU-*n* ($n = 1-6$). The mixture of $Cu(NO_3)_2\cdot 3H_2O$ (0.24 g, 1mmol) and $H_4SiW_{12}O_{40}\cdot nH_2O$ (0.2 g) for **1**, $H_4GeW_{12}O_{40}\cdot nH_2O$ (0.2 g) for **2**, $H_3PW_{12}O_{40}\cdot nH_2O$ (0.2 g) for **3**, $H_4SiMo_{12}O_{40}\cdot nH_2O$ (0.2 g) for **4**, $H_3PMo_{12}O_{40}\cdot nH_2O$ (0.2 g) for **5**, and $H_3AsMo_{12}O_{40}\cdot nH_2O$ (0.2 g) for **6** in distilled water (10 mL) was stirred for 20 min, and then H_3BTC (0.21 g, 1mmol) and $(CH_3)_4NOH$ (0.09 g, 1 mmol) were added in succession. We continued stirring the mixture for 30 min at room temperature. The turbid mixture (pH = 2−3) was sealed in a Teflon-lined autoclave and heated at 180 °C for 24 h, followed by slow cooling to room temperature. Blue or green octahedral crystals were then collected.

(11) (a) Chen, B.; Eddaoudi, M.; Hybe, S. T.; O'Keeffe, M.; Yaghi, O. M. *Science* **2001**, *291*, 1021. (b) Férey, G. *Chem. Mater.* **2001**, *13*, 3084. (c) Rowsell, J. L. C.; Yaghi, O. M. *J. Am. Chem. Soc.* **2006**, *128*, 1304. (d) Kitagawa, S.; Kitaura, R.; Noro, S. *Angew. Chem., Int. Ed.* **2004**, *43*, 2334. (e) Huang, X.-C.; Lin, Y.-Y.; Zhang, J.-P.; Chen, X.-M. *Angew. Chem., Int. Ed.* **2006**, *45*, 1557. (f) Cheng, X.-N.; Zhang, W.-X.; Chen, X.-M. *J. Am. Chem. Soc.* **2007**, *129*, 15738. (g) Zhang, M.-B.; Zhang, J.; Zheng, S.-T.; Yang, G.-Y. *Angew. Chem., Int. Ed.* **2005**, *44*, 1385. (h) Xie, L.-H.; Liu, S.-X.; Gao, C.-Y.; Cao, R.-G.; Cao, J.-F.; Sun, C.-Y.; Su, Z.-M. *Inorg. Chem.* **2007**, *46*, 7782.

(12) Chen, B.; Ockwig, N. W.; Millward, A. R.; Contreras, D. S.; Yaghi, O. M. *Angew. Chem., Int. Ed.* **2005**, *44*, 4745.

(13) Chen, B.; Liang, C.; Yang, J.; Contreras, D. S.; Clancy, Y. L; Lobkovsky, E. B; Yaghi, O. M.; Dai, S. *Angew. Chem., Int. Ed.* **2006**, *45*, 1390.

(14) Horike, S.; Dincă, M.; Tamaki, K.; Long, J. R. *J. Am. Chem. Soc.* **2008**, *130*, 5854.

(15) Horcajada, P.; Serre, C.; Vallet-Regí, M.; Sebban, M.; Taulelle, F.; Férey, G. *Angew. Chem., Int. Ed.* **2006**, *45*, 5974.

(16) Fang, Q.-R.; Zhu, G.-S.; Jin, Z.; Ji, Y.-Y.; Ye, J.-W.; Xue, M.; Yang, H.; Wang, Y.; Qiu, S.-L. *Angew. Chem., Int. Ed.* **2007**, *46*, 6638.

(17) Alkordi, M. H.; Liu, Y.; Larsen, R. W.; Eubank, J. F.; Eddaoudi, M. *J. Am. Chem. Soc.* **2008**, *130*, 12639.

(18) (a) Hagrman, D.; Hagrman, P. J.; Zubieta, J. *Angew. Chem., Int. Ed.* **1999**, *38*, 3165. (b) Zheng, L. M.; Wang, Y. S.; Wang, X. Q.; Korp, J. D.; Jacobson, A. J. *Inorg. Chem.* **2001**, *40*, 1380. (c) Inman, C.; Knaust, J. M.; Keller, S. W. *Chem. Commun.* **2002**, 156. (d) Yang, L.; Naruke, H.; Yamase, T. *Inorg. Chem. Commum.* **2003**, *6*, 1020. (e) Férey, G.; Mellot-Draznieks, C.; Serre, C.; Millange, F.; Dutour, J.; Surblé, S.; Margiolaki, I. *Science* **2005**, *309*, 2040. (f) Wei, M.; He, C.; Hua, W.; Duan, C.; Li, S.; Meng, Q. *J. Am. Chem. Soc.* **2006**, *128*, 13318. (g) Zhao, X.; Liang, D.; Liu, S.; Sun, C.; Cao, R.; Gao, C.; Ren, Y.; Su, Z. *Inorg. Chem.* **2008**, *47*, 7133.

(19) Maksimchuk, N. V.; Timofeeva, M. N.; Melgunov, M. S.; Shmakov, A. N.; Chesalov, Yu, A.; Dybtsev, D. N.; Fedin, V. P.; Kholdeeva, O. A. *J. Catal.* **2008**, *257*, 315.

(20) (a) Rosi, N. L.; Eddaoudi, M.; Kim, J.; O'Keeffe, M.; Yaghi, O. M. *Angew. Chem., Int. Ed.* **2002**, *41*, 284. (b) Rosi, N. L.; Eckert, J.; Eddaoudi, M.; Vodak, D. T.; Kim, J.; O'Keeffe, M.; Yaghi, O. M. *Science* **2003**, *300*, 1127. (c) Serre, C.; Millange, F.; Surblé, S.; Férey, G. *Angew. Chem., Int. Ed.* **2004**, *43*, 6285. (d) Liu, Y.; Eubank, J. F.; Cairns, A. J.; Eckert, J.; Kravtsov, V. C.; Luebke, R.; Eddaoudi, M. *Angew. Chem., Int. Ed.* **2007**, *46*, 3278.

(21) Deltcheff, C. R.; Fournier, M.; Franck, R.; Thouvenot, R. *Inorg. Chem.* **1983**, *22*, 207, and reference cited therein.

(22) Chui, S. S.-Y.; Lo, S. M.-F.; Charmant, J. P. H.; Orpen, A. G.; Williams, L. D. *Science* **1999**, *283*, 1148.

The entire yields for **1**−**6**: 60−80% based on Cu. IR (KBr, cm^{-1}) for **1**: 1652, 1484, 1450, 1374, 1108, 1015, 976, 924, 885, 809, 792, 754, 729, 494; for **2**: 1643, 1590, 1448, 1380, 1102, 969, 912, 828, 749, 713, 481; for **3**: 1651, 1484, 1450, 1374, 1107, 1081, 986, 945, 897, 825, 795, 755, 729, 495; for **4**: 1651, 1483, 1451, 1417, 1375, 1109, 954, 906, 808, 793, 755, 729, 494; for **5**: 1649, 1453, 1373, 1109, 1064, 967, 880, 816, 753, 727, 495; and for **6**: 1644, 1592, 1445, 1382, 1104, 997, 918, 804, 787, 757, 716, 482. Elemental Anal. Calcd (Found %) for $C_{80}H_{133}N_2O_{130}Cu_{12}SiW_{12}$ (**1**): C, 15.50 (15.23); H, 2.16 (2.26); N, 0.45 (0.40); Si, 0.45 (0.39); Cu, 12.30 (12.47); W, 35.59 (35.90); for $C_{80}H_{133}N_2O_{130}Cu_{12}GeW_{12}$ (**2**): C, 15.39 (15.19); H, 2.15 (2.24); N, 0.45 (0.41); Ge, 1.16 (1.27); Cu, 12.21 (12.00); W, 35.34 (35.77); for $C_{80}H_{123}N_2O_{125}Cu_{12}PW_{12}$ (**3**): C, 15.72 (15.56); H, 2.03 (2.14); N, 0.46 (0.42); P, 0.51 (0.47); Cu, 12.48 (12.69); W, 36.10 (35.71); for $C_{80}H_{133}N_2O_{130}Cu_{12}SiMo_{12}$ (**4**): C, 18.68 (18.97); H, 2.60 (2.71); N, 0.54 (0.51); Si, 0.54 (0.41); Cu, 14.82 (14.61); Mo, 22.38 (22.03); for $C_{80}H_{113}N_2O_{120}Cu_{12}PMo_{12}$ (**5**): C, 19.34 (19.09); H, 2.27 (2.18); N, 0.56 (0.52); P, 0.62 (0.71); Cu, 15.35 (15.14); Mo, 23.18 (23.47); and for $C_{80}H_{113}N_2O_{120}Cu_{12}AsMo_{12}$ (**6**): C, 19.17 (19.40); H, 2.26 (2.17); N, 0.56 (0.53); As, 1.50 (1.75); Cu, 15.22 (15.38); Mo, 22.98 (22.61).

Preparation of $[Cu_{12}(BTC)_8][H_3PW_{12}O_{40}]$ (NENU-3a). The as-synthesized blue octahedral crystals of **3**, which had an exact weight of 2.0012 g, were placed in a high vacuum oven at 200 °C for 12 h with a weight loss of 13.41% (calcd 13.35% for all of the water molecules and $(CH_3)_4N^+$ cations). Then the solvent-free phase $[Cu_{12}(BTC)_8][H_3PW_{12}O_{40}]$ (**3a**) was obtained as black crystals (1.7330 g). IR: 1652, 1450, 1374, 1104, 1079, 980, 903, 825, 795, 756, 729, and 494 cm^{-1}. Elemental Anal. Calcd (Found %) for $C_{72}H_{27}O_{88}Cu_{12}PW_{12}$: C, 16.32 (16.48); H, 0.51 (0.49); P, 0.58 (0.47); Cu, 14.39 (14.99); and W, 41.63 (42.02). The presence of three acidic protons in **3a** was confirmed by acid−base titration.

X-Ray Structure Analysis. Single-crystal diffractometry was conducted on a Bruker Smart Apex CCD diffractometer with Mo Kα monochromated radiation (λ = 0.710 73 Å) at room temperature. The linear absorption coefficients, scattering factors for the atoms, and anomalous dispersion corrections were taken from the International Tables for X-Ray Crystallography. Empirical absorption corrections were applied. The structures were solved by using the direct method and refined through the full-matrix least-squares method on F^2 using SHELXS-97. Anisotropic thermal parameters were used to refine all non-hydrogen atoms, except for crystallization water oxygen and $(CH_3)_4N^+$ cations. The hydrogen atoms attached to carbon positions were placed in geometrically calculated positions. Approximately 20−30 crystallization water molecules were estimated by thermogravimetry, and only partial oxygen atoms of water molecules were achieved with the X-ray structure analysis. The crystal data and structure refinement results of compounds **1**−**6** are summarized in Table S1. Selected bond lengths and angles are listed in Tables S2 and S3, respectively. CCDC reference numbers 686793, 686794, 686795, 686796, 686797, and 686798 are listed for **1**−**6**.

Acid−Base Titration and Back Titration. The amount of acidic protons in **3** and **3a** were determined through acid−base titration. Crystalline solid **3** (0.5193 g) or **3a** (0.5102 g) was placed in 50 mL of carbonate-free, 0.0085 M sodium hydroxide solution, which was standardized by titrations with a standard potassium hydrogen phthalate solution. The mixture was sealed and stirred for 10 h at room temperature, filtering off the solids, and the filtrate was back-titrated using 0.0136 M hydrochloric acid, which was standardized by titrations with a standardized sodium hydroxide solution. Then the number of acidic protons of **3** (0.18 mmol g^{-1}) and **3a** (0.57 mmol g^{-1}) could be calculated from the consumed sodium hydroxide amount.

N_2 Sorption Properties. The samples of 0.086 g for HKUST-**1** and 0.108 g for evacuated NENU-**3a** were used for the gas sorption measurements at 77 K. To remove guest solvent molecules from the framework, the as-synthesized crystal HKUST-**1** was heated overnight under vacuum at 150 °C. Before the measurement was taken, both samples were vacuumed again by using the "outgas" function of the surface area analyzer for 10 h (at 150 °C for HKUST-1, and 200 °C for **3a**).

Hydrolysis of Esters Catalyzed by 3 and 3a. Hydrolysis reactions were performed for five kinds of esters: methyl acetate, ethyl acetate, methyl benzoate, ethyl benzoate, and 4-methyl-phenyl propionate. A standard hydrolysis procedure was performed in a bath reactor (a three-neck Pyrex flask ca. 120 cm^3) with a water cooler condenser, a thermometer, and a glass tube to extract the solution. Methyl acetate and ethyl acetate hydrolysis were carried out using a 5 wt% of the aqueous (30 cm^3, 20.00 mmol of methyl acetate, or 16.90 of mmol ethyl acetate was included). The solubility of the methyl benzoate, ethyl benzoate, and 4-methyl-phenyl propionate in water is very low, so the hydrotropic solvent acetonitrile was used to increase their solubility. The methyl benzoate (4.40 mmol), ethyl benzoate (4.00 mmol), and 4-methyl-phenyl propionate (3.65 mmol) were dissolved in 5 mL of acetonitrile and then diluted with water to a 30 mL aqueous solution (2 wt%), and a transparent homogeneous solution was obtained. The weight of solid catalysts **3** and **3a** was 0.20 g. The reaction temperature was raised immediately to 60 °C for methyl acetate and ethyl acetate or 80 °C for methyl benzoate, ethyl benzoate, and 4-methyl-phenyl propionate. The suspension was stirred vigorously for 8 h. Aliquots of the reaction mixture were periodically withdrawn with a syringe over the course of the reaction. The products were analyzed with GC or GC−MS. After the reaction, the catalyst was separated by filtration subjected to a recycling experiment after full washing and heated at 200 °C for 6 h under reduced pressure.

The catalytic activity of the catalyst for the hydrolysis of ethyl acetate was estimated from the conversion of ethyl acetate at 2 h (about 7% for **3** and about 25.4% for **3a**) and normalized by the unit time and catalyst amount. The catalytic activity is expressed in two ways:[23] as a $k1$ (μmol $g_{cat.}^{-1}$ min^{-1}) rate on the basis of catalyst weight and a $k2$ (mmol $mol_{acid.}^{-1}$ min^{-1}) rate on the basis of acid amount. They are given by

$$k1 = (CN)/(tm_{cat}) \quad (1)$$

$$k2 = k1/\text{acid amount} \quad (2)$$

where C designates the conversion that was defined as (amount of alcohol formed)/(amount of ester added); N is the molar amount of ester added; t is the reaction time; and m_{cat} denotes the weight of the catalyst. The acid amounts of the compounds adopted in the present paper (**3**, 0.18 mmol g^{-1}; **3a**, 0.57 mmol g^{-1}) were measured by acid−base titration, which is consistent with the total H^+ content calculated from the chemical composition.

Results and Discussion

Synthesis, Crystal Structures, and Compound Stability. NENU-**1** through **6** were produced by heating various Keggin POMs, copper nitrate, H_3BTC, and $(CH_3)_4NOH$ at 180 °C for 24 h. The $(CH_3)_4NOH$ performs two functions: H_3BTC deprotonation and charge compensation. This tailor-made approach permitted one-step framework construction and POM encapsulation. The fine crystals obtained through this method are suitable for X-ray crystallography. Although compounds **3** and **4** could be obtained by the previously reported method,[18d] we found that our procedure can markedly increase the quality and quantity of crystals compared to prior syntheses. Our method also has even extensiveness because almost all of the Keggin-type POMs can be introduced into this system. The textural characteristics of these compounds are well-defined, and the loaded amount of POMs can also be unambiguously confirmed (**1**, 46.4%; **2**, 46.7%; **3**, 47.1%; **4**, 35.4%; **5**, 35.5%; **6**, 37.2%),

(23) Kimura, M.; Nakato, T.; Okuhara, T. *Appl. Catal., A* **1997**, *165*, 227.

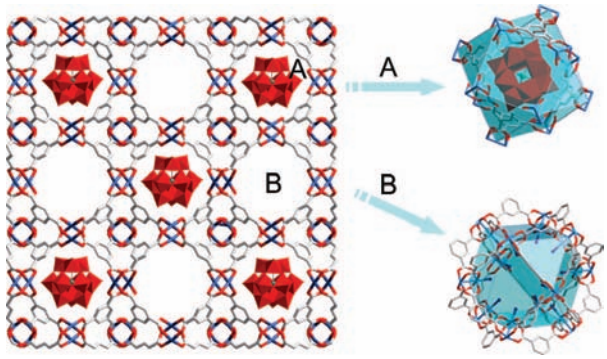

Figure 1. View of a (001) sheet with two kinds of pores, A and B, in **NENU-*n*** (***n*** = **1**−**6**). The Cu-BTC framework and Keggin polyanions are represented by wireframe and polyhedral models. Blue, red, and gray represent Cu, O, and C, respectively.

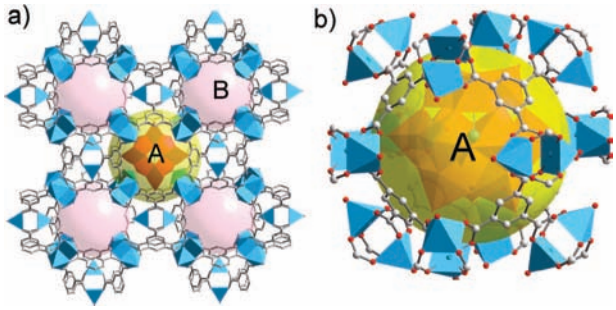

Figure 2. Components of the crystal structures of **NENU-*n*** (***n*** = **1**−**6**): (a) a cube of five truncated-octahedral cages sharing square faces; (b) the pore A accommodating the Keggin polyanion, Cu2-cluster (blue polyhedra), Keggin polyanion (red polyhedra), C (gray), and O (red). All H atoms and solvent molecules are omitted for clarity.

which differs from the most ill-defined POMs-supported catalysts. These loaded amounts exceed the most traditional, POM-supported catalysts.

The X-ray diffraction study reveals that NENU-**1** through **6** are isomorphous and that Keggin-type POMs with different charges as guests have been introduced into an open porous system in which the paddle-wheel unit Cu_2-clusters are connected through the BTC ligands into a three-dimensional (3,4)-connected cubic network (Figures S1 and S2 in the Supporting Information). Interestingly, this host framework is isostructural with the famous compound HKUST-1 reported by Chui et al.,[22] which indicates that the well-defined reaction conditions for the in situ preparation of SBUs in MOFs were still available in this system. One structural feature of these compounds is that there are two kinds of pores (A and B), with free diameters of ca. 13 and 10 Å, accessible through the windows for ca. 11 and 9.3 Å, respectively (Figure 1). Pore A, which accommodates the Keggin anions, has a cuboctahedral shape in which the BTC groups define the eight triangular planes of cuboctahedral, and Cu_2-clusters locate 12 vertices. Pore B provides a cuboctahedral space, but the coordinated water molecules of copper point toward the inside of the pore, and as a result, the Keggin anion cannot be incorporated into pore B. Pores A and B are arranged alternately in the face-centered cubic lattice. The six open squares of the cubocathedral pore A are connected to the adjacent six pore B (Figure 2).

The crystallization water molecules and $(CH_3)_4N^+$ cations are located in the B pores. The total potential solvent area volumes of these compounds, calculated with *PLATON*,[24] are ∼24−30%. One trait of these compounds is reversible color changes related to dehydration and rehydration (as shown in Figure S4 in the Supporting Information). In compounds **1**−**6**, the physically and chemically bound water molecules are easily removed from the host material by heating. The as-synthesized materials are blue (for the W series) or green (for the Mo series), while the dehydrated materials are black. Rehydration materials restore the original color, indicating the coordination of water with the copper ions. This phenomenon revealed that the unique attributes of the host matrix were maintained in these compounds. Another significant feature of these compounds is polyanion protonation. The host framework of these compounds is a charge-neutral, X-ray crystallography combined with the C, H, N elemental analyses, atomic absorption spectra, and TG analyses, which confirmed that only two $(CH_3)_4N^+$ cations existed in these compounds; no other cations could be observed. Keggin anion protonation is necessary for charge compensation. But no protonation site could be determined by X-ray diffraction or bond valence analysis because the anions are disordering (Figure S1 in the Supporting Information), something that is often observed in POM compounds.[25] Given the high nucleophilicity of the terminal and the bridging oxygen atoms of POMs, it is reasonable to believe that these atoms were protonated. The presence of acid protons in **3** and **3a** was also confirmed by acid−base titration (vide infra).

The essential properties of solid catalysts are the stability of the active component with respect to leaching and other transformations, the persistence of the porous structure, and toleration for thermal or acid−base conditions. Compounds **1**−**6** were stable for months under air atmosphere, and no efflorescence was observed. These compounds in 0.02 M sodium hydroxide solution, 0.02 M hydrochloric solution, or common organic solvents (methanol, ethanol, acetonitrile, acetone, chloroform, and DMF) were stirred for 10 h at 80 °C and showed no compound dissolution, framework decomposition, or POM leaching, as evidenced by the UV−vis, IR, and XRD patterns. Moreover, these compounds were exposed in deionized water for 3 months, and aliquots of the solution, which were withdrawn periodically, showed no evidence of POM leaching on the research time scale monitored by UV−vis. The IR and XRD of the marinated compounds match that of the as-synthesized samples, confirming the maintenance crystalline framework. The TG curves of compounds **1**−**6** indicated a weight loss of 13.35−17.48% (calcd 13.31−17.60%), corresponding to the loss of all of the water molecules and $(CH_3)_4N^+$ cations by ∼250 °C. An obvious plateau of ∼150−250 °C can be observed for these compounds, indicating their high thermal stability (see Figure S5 in the Supporting Information). The porosity of **3a** was also investigated. The N_2 sorption isotherm of **3a** (Figure S6 in the Supporting Information) reveals a type I behavior indicative of a microporous material, although the sorption capacity of **3a** decreases when compared with the host material HKUST-1, which was prepared according to the literature[23] under identical conditions. The total amount uptake of **3a** was 142 $cm^3\ g^{-1}$ (258 $cm^3\ g^{-1}$ for HKUST-1). By applying the Langmuir equations, we were able to estimate the Langmuir

(24) Spek, A. L. *PLATON*; Utrecht, The Netherlands, 2000.
(25) (a) Evans, H. T.; Pope, M. T. *Inorg. Chem.* **1984**, *23*, 501. (b) Galán-Mascarús, J. R.; Giménez-Saiz, C.; Triki, S.; Gómez-García, C. J.; Coronado, E.; Ouahab, L. *Angew. Chem., Int. Ed. Engl.* **1995**, *34*, 1460. (c) Coronado, E.; Galán-Mascarós, J. R.; Giménez-Saiz, C.; Gómez-García, C. J.; Triki, S. *J. Am. Chem. Soc.* **1998**, *120*, 4671. (d) Ishii, Y.; Takenaka, Y.; Konishi, K. *Angew. Chem., Int. Ed.* **2004**, *43*, 2702. (e) Lisnard, L.; Dolbecq, A.; Mialane, P.; Marrot, J.; Codjovi, E.; Sécheresse, F. *Dalton Trans.* **2005**, 3913.

surface area of **3a** as 460 $m^2\ g^{-1}$ (1116 $m^2\ g^{-1}$ for HKUST-1). These results indicate that **3a** still had porosity, even after the introduction of POMs into the host framework, which is consistent with the crystal structure of **3a** (only pore A is occupied by polyanion and the empty pore remains able to host other species). All of these results definitely indicate that these materials are highly stable.

Characterization of 3a and Esters Hydrolysis Catalyzed by 3a. The as-synthesized crystalline solid of **3** was placed in a high vacuum oven at 200 °C for 12 h with a 13.41% weight loss (calcd 13.35% for 37 water molecules and 2 $(CH_3)_4N^+$ cations) to obtain the evacuated solid. The IR spectra of the evacuated solid showed the bands were characteristic of the matrix and polyoxometalate, indicating that the molecular structures of the constituents were retained. The elimination of $(CH_3)_4N^+$ cations was indicated by the disappearance of the C−H stretching peak at 1484 cm^{-1} in the IR spectrum (Figure S7 in the Supporting Information). The XRD pattern of evacuated material was compared with that of as-synthesized **3**, as well as the simulated powder pattern obtained from the single-crystal model of **3** (Figure S8 in the Supporting Information). The good agreement of the peaks in all of the diagrams demonstrated that the framework structure was retained upon complete removal of the water molecules and $(CH_3)_4N^+$ cations. For the charge balance, the decomposition of $(CH_3)_4N^+$ cations must leave the H^+ on the polyanions. The presence of three acid protons in **3a** was confirmed by acid−base titration. A formula of $[Cu_{12}(BTC)_8][H_3PW_{12}O_{40}]$ (NENU-**3a**) was further confirmed by the elemental analysis.

The amount of acidic protons of **3a** was measured by acid−base titration to evaluate the catalytic activity per acidic proton. The highly stable framework and high immobility of POMs limit the determination of the proton content by releasing the POMs. Because the OH^- can diffuse into the framework to neutralize the H^+ on polyanions, a sodium hydroxide solution was used to permeate the compound, and then the filtrate was back-titrated using standardized hydrochloric acid to determine the residual content of the OH^-, thus enabling us to calculate the amount of acidic protons in **3a**. The results indicated that **3a** had 5.7×10^{-4} mol g^{-1} of acidic protons, which corresponds to three acidic protons per polyanion. The amount of protons in **3** was determined for the sake of comparison and yielded 1.8×10^{-4} mol g^{-1} of acidic protons, which corresponds to one acidic proton per polyanion. These results demonstrate that the evacuated **3a** exposes more acid active sites than **3**, which is favorable for catalysis.

The hydrolysis of ester in excess water was chosen as a test reaction to assess the acid catalysis of these new materials. The well-known $H_3PW_{12}O_{40}$ species is the strongest Brønst acid in the Keggin series.[3] Thus, for a typical experiment, **3a** containing the $H_3PW_{12}O_{40}$ species was chosen as a catalyst for esters hydrolysis. Table 1 lists the catalytic activities of **3a** for ethyl acetate hydrolysis in excess water (with rates based on catalyst weight and acid amount, respectively) and also those of **3** and other acid catalysts under the same reaction conditions for comparison. The activities were estimated from the conversion of ethyl acetate after reaction for 2 h (about 25.4% for **3a**). As shown in Table 1, the activity of **3a** (per unit weight) was far superior to most inorganic solid acids and comparable to organic solid acids. What is notable here is that the specific activity of **3a** (per unit of acid) was the most active among all the acids. It was ∼3 to 7 times higher than that of H_2SO_4, $H_3PW_{12}O_{40}$, SO_4^{2-}/ZrO_2, Nafion-H, and Amberlyst-15. The specific activity of **3a** also exceeded the best prior results of 275 mmol $mol_{acid.}^{-1}$ min^{-1} obtained by H_3PW_{12} immobilized in organomodified mesoporous silica.[26] In addition, the conversion of ethyl acetate was gradually enhanced by an increase in the reaction period, which reached a maximum of >95% at ∼7 h in **3a**. The relatively long reaction time may be caused by the time-consuming diffusion. It can also be observed that the evacuated **3a** showed higher catalytic activity than **3** (the conversion of **3** is only about a quarter of **3a** under the same conditions). In this case, only ethanol and acetic acid were formed as the reaction products, suggesting that the investigated reaction tends toward the formation of this alcohol and carboxylic acid. The control reactions implied that the observed catalytic behavior is unique to **3a** (MOF impregnated with POMs): no reaction in the absence of catalysts; no reaction in the presence of only the solid matrix HKUST-1 (no POMs); and low conversion in the presence of HKUST-1 and $H_3PW_{12}O_{40}$ (simply mixed), which can be attributed to the homogeneous catalysis caused by $H_3PW_{12}O_{40}$. All of these results confirmed that the extracted **3a** showed extremely high catalytic activity, and there was no deactivation of the acid sites by water. To probe the catalyst's selectivity, the substrates with increasing dimension were tested. As illustrated in Figure 3, the conversion of methyl acetate and ethyl acetate molecules with dimensions of 4.87×3.08 Å[2][27] and 6.11×3.11 $Å^2$, respectively, reached ∼64% after 5 h. In contrast, the conversion of ethyl benzoate with molecular dimensions of 8.96×4.65 $Å^2$ was reduced to below 20% under similar conditions. The conversion of 4-methyl-phenyl propionate, a larger ester with dimensions of 10.61×4.04 $Å^2$, was still below 1% after 24 h.

The catalytic activity and selectivity of **3a** seem to depend on the size and accessibility of the substrates for surface pores. The polyanions are ∼1 nm in diameter and almost totally cram

Table 1. Activity of Catalysts for Ethyl Acetate Hydrolysis in Water

catalyst	acid amount (mmol g^{-1})	catalytic activity per cat. weight (μmol $g_{cat.}^{-1}$ min^{-1})	per acid amount (mmol $mol_{acid.}^{-1}$ min^{-1})
(Solid Oxides)			
NENU-**3a**[a]	0.57[b]	178.9	313.8
NENU-**3**[a]	0.18[b]	49.3	273.9
PW/C_8-AP-SBA[26]	0.091	25.1	275.0
$Cs_{2.5}H_{0.5}PW_{12}O_{40}$[23]	0.15	30.1	200.6
$Cs_3PW_{12}O_{40}$[23]	0.0	0.0	0.0
SO_4^{2-}/ZrO_2[23]	0.20	25.5	127.5
H-ZSM-5[23]	0.39	27.6	70.8
Nb_2O_5[23]	0.31	4.0	12.9
HY zeolite[23]	2.60	0.0	0.0
(Organic Resins)			
Nafion-H resin[23]	0.80	161.9	202.3
Amberlyst-15[23]	4.70	193.6	41.2
(Liquid Acids)			
$H_3PW_{12}O_{40}$[23]	1.0	70.4	70.4
H_2SO_4[23]	19.8	911.9	46.1
(MOF)			
HKUST-1	0.0	0.0	0.0

[a] Reaction conditions: 60 °C, a 5 wt% 30 mL aqueous solution of ethyl acetate (16.9 mmol), catalyst weight 0.20 g, conversion at 2 h 25.4% for **3a**, 7.0% for **3**. [b] Measured by acid−base titration, the results are consistent with the total H^+ content calculated from the chemical composition.

(26) Inumaru, K.; Ishihara, T.; Kamiya, Y.; Okuhara, T.; Yamanaka, S. *Angew. Chem., Int. Ed.* **2007**, *46*, 7625.
(27) The dimensions given represent maximal cross-sections for the molecules, as determined based on the CIF file coming from Cambridge Crystallographic Data Centre.

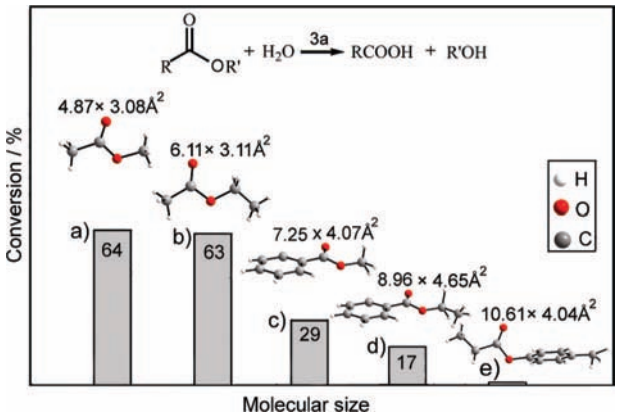

Figure 3. Results for the hydrolysis of ester in the presence of NENU-**3a**: (a) methyl acetate; (b) ethyl acetate; (c) methyl benzoate; (d) ethyl benzoate; and (e) 4-methyl-phenyl propionate. The reactions were performed with 5 wt% 30 mL aqueous solution for (a) and (b) at 60 °C and 2 wt% 30 mL aqueous solution for (c)−(e) at 80 °C, respectively; catalyst weight 0.20 g; reaction time 5 h.

pore A. Pore B communicates with pore A through the six open square windows. It was easily observed from the crystal structure that the inside environment of channels is hydrophilic, while phenyl (BTC) increases the hydrophobicity of surface pores around the polyanions. It is thereby reasonable that the reactants with smaller sizes and higher hydrophilicity, such as methyl acetate and ethyl acetate, can diffuse swiftly through the pores. The catalytic reactions take place in the pores, and then the products diffuse into the solution. In this case, substrate accessibility for the surface pores is less important and, as a result, the methyl acetate and ethyl acetate conversions are almost independent of the number of carbon atoms. In contrast, the substrates with larger sizes and higher hydrophobicity (more phenyl) are not readily diffused through the pores, but they may adsorb onto the surface pores containing Keggin complexes, and the acidic protons on the polyanions catalyze the reaction at the surface of the pores. In this case, substrate accessibility for the surface pores is likely to dominate. Although methyl benzoate, ethyl benzoate, and 4-methyl-phenyl propionate have similar sizes in a certain dimension, they have shown different conversions, possibly due to their varied accessibility for the surface of the pore. The attribute that protected the acid sites from poisoning by water, while allowing the reactant molecules ready access to the acidic sites on POMs, is responsible for their highly catalytic activity. In addition, the high POM loading (47%) and the well-dispersed POMs at the molecular level may also serve as advantages.

The solids of **3a** are readily separated from the reaction system by simple filtration, which is a unique feature of heterogeneous, solid, immobilized catalysts that allows for studies of a catalyst's recyclability. Indeed, **3a** is recyclable under the reaction conditions up to at least the 15th cycle without losing its reactivity and selectivity. Each cycle was run for 8 h, and then **3a** was isolated, washed with methanol, and dried at 200 °C. No POM leaching was observed in the UV−vis spectrum of the product solution. The XRD patterns of **3a** before and after the reactions remained almost unchanged, indicating the high stability and immobility of **3a** (Figure S8 in the Supporting Information). The solution became completely inactive after the solid catalyst was removed. This indicates that the catalytic process is truly heterogeneous and occurs on the solid rather than in solution.

Conclusion

In summary, we developed a strategy to prepare a series of crystalline materials in which the protonated POMs are included in the host matrix of an MOF through hydrothermal reaction. The hydrolysis of esters catalyzed by compound **3a** as heterogeneous acid catalysts was investigated for the first time and showed high activity. The results confirmed that these compounds have great potential for use as solid catalysts. They possess the following excellent characteristics, which are comparable to the conventional, POM-supported catalysts: unambiguous X-ray crystallography, which confirms their texture; good dispersion of POMs at the molecular level, which prohibits conglomeration; high immobilization of POMs, which overcomes catalyst leaching and deactivation; and their highly stable crystalline framework, which allows for catalyst recycling. The approaches presented here show that designing a novel material with a cooperative function based on the MOFs and POMs is a promising strategy. Work is underway to explore the catalytic mechanism in greater detail and expand this approach to other transformations with suitable host frameworks and polyanions.

Acknowledgment. This work was supported by the National Science Foundation of China (Grant No. 20871027), the Program for New Century Excellent Talents in University (NCET-07-0169), and the Program for Changjiang Scholars and Innovative Research Team in University.

Supporting Information Available: Further details on the crystal structures of **1**−**6** (CIF), IR, TG, PXRD patterns, and N_2 gas sorption isotherms. This material is available free of charge via the Internet at http://pubs.acs.org.

JA807357R